The geology and petrogenesis of the Capitan Pluton, New Mexico

Michael S. Allen and Virginia T. McLemore

1991, pp. 115-127. https://doi.org/10.56577/FFC-42.115

in:

Geology of the Sierra Blanca, Sacramento, and Capitan Ranges, New Mexico, Barker, J. M.; Kues, B. S.; Austin, G. S.; Lucas, S. G.; [eds.], New Mexico Geological Society 42 nd Annual Fall Field Conference Guidebook, 361 p. https://doi.org/10.56577/FFC-42

This page is intentionally left blank to maintain order of facing pages.

THE GEOLOGY AND PETROGENESIS OF THE CAPITAN PLUTON, NEW MEXICO

MICHAEL S. ALLEN[1] and VIRGINIA T. McLEMORE[2]
[1]U.S. Geological Survey, 210 East 7th St., Tucson, Arizona 85705; [2]New Mexico Bureau of Mines and Mineral Resources, Socorro, New Mexico 87801

Abstract—The elongate Capitan pluton of the Lincoln County porphyry belt (LCPB) is the largest exposed Tertiary intrusion in New Mexico (280 km^2). Study of 1340 m of vertical exposure within the Capitan pluton reveals it to be a zoned, hypabyssal, alkali feldspar granite with discordant and concordant intrusive relationships with Paleozoic country rock. The roof zone (west end) of the pluton consists of a high-silica (75.0%), micromiarolitic, granophyric aplite, enriched in Ta, Nb, Th, Y and HREE, and depleted in Fe, Mg, Ca, Al, Na + K, Ti, P, Zr, Sr, Ba, Co, Ni and LREE relative to a lower silica (71.2%), amphibole, biotite, subsolvus, fine-grained, granite-porphyry core (east end). Data are consistent with fractionation of apatite, titanite, zircon and feldspar to produce the observed zonation. Micromiarolitic samples display severe depletion of Ca, Fe, LREE, U and Th consistent with mobilization of these elements into an aqueous phase, which resulted in formation of the Capitan iron skarn deposit, and thorium- and REE-bearing quartz veins. Fractionation in a high-level chamber to produce the zoning of the Capitan granite is problematic, due to its rapid crystallization. A model of flow differentiation is favored. The igneous centers of the LCPB were controlled by two major structures: the north-south Pedernal arch and the east-west Capitan lineament. These crustal flaws allowed leakage of magmas at different times, depending on fracture orientation and changes in tectonic stress regime. Igneous activity along the Pedernal trend consists of pre-rift (38.2–36.5 Ma) alkalic complexes, and early-rift (30–26.5 Ma) syenites and granites. Along the Capitan lineament, bimodal mafic alkalic and granite intrusions such as the Capitan pluton were emplaced during early rifting from 28 to 26.5 Ma. Contemporaneity of mafic alkalic and granitic magmatism along the Capitan lineament suggests that an areally extensive, early rift, mantle-melting event caused melting of the lower crust, generating granitic magmas. Isotope systematics (Sr, Nd, O) and REE patterns are consistent with derivation of the Capitan pluton from a metaigneous lower crustal source.

INTRODUCTION

The Capitan pluton is the largest exposed Tertiary pluton in New Mexico, with an outcrop area of approximately 280 km^2 and an estimated exposed volume of 300 km^3. It is one of several Tertiary igneous centers in south-central New Mexico, which were referred to by Kelley and Thompson (1964) as the Lincoln County porphyry belt (LCPB). The pluton is also the most prominent igneous feature of the Capitan lineament, a major east-west alignment of structures and igneous features that traverses New Mexico perpendicular to the Rio Grande rift (Kelley and Thompson, 1964). Until recently, the Capitan pluton has received little study.

Early investigations of the pluton included reconnaissance petrologic studies and regional geologic mapping (Sidwell, 1946; Patton, 1951; Kelley and Thompson, 1964; Kelley, 1971), or focused on the mineral deposits associated with the pluton (Sheridan, 1947; Kelley, 1949, 1952; Griswold, 1959, 1964; Harrer and Kelley, 1963; Butler, 1964; McLemore, 1983; Tuftin, 1984; McLemore et al., 1988a, b). These early workers noted the pluton's apparent uniform fine-grained granitic character, but petrographic and chemical analyses were limited (Butler, 1964; Kelley, 1971). This apparent uniform fine-grained texture, considered together with the pluton's large size and elongate shape, presented an enigma to geologists considering its origin (Kelley, 1971).

Allen (1988) determined the pluton to be a single-phase, but vertically and laterally zoned, granite intrusion. The pluton's setting and vertical exposure provide an unusual opportunity to study a well-preserved, compositionally zoned, crystallized magma body, and to make inferences about the magmatic processes operative in its formation. This report is a synthesis of recent work aimed at describing the textural and compositional variation of the Capitan pluton, and constraining the processes involved in its generation and resultant zoning. A comparison of the petrogenesis of the Capitan pluton to other igneous centers of the LCPB is useful in understanding the complex Tertiary igneous history of the Ruidoso region.

GEOLOGIC SETTING

Regional tectonic setting

Though the Capitan pluton is the focus of this report, its ultimate origin is perhaps best understood by examining its relationship to the other Tertiary igneous rocks of the LCPB and the tectonic processes and features controlling their distribution. A more thorough discussion of the LCPB is presented by Allen and Foord (1991b, this volume).

The Capitan pluton is one of several Tertiary igneous centers in east-central New Mexico, which were referred to by Kelley and Thompson (1964) as the Lincoln County porphyry belt (LCPB), because of the porphyritic textures displayed by many of the lithologies of these centers. Due to the alkalic affinity of the rocks of the LCPB (Thompson, 1972; Giles and Thompson, 1972; Moore et al., 1985; Allen and Foord, 1991b, this volume), the LCPB may be considered part of the Rocky Mountain alkalic province (RMAP) (Carmichael et al., 1974). The RMAP includes Tertiary alkalic igneous centers distributed along the Rocky Mountain front from Canada into Mexico (Fig. 1). Igneous activity in the RMAP is concentrated along the boundary between the stable craton (Great Plains) and the Laramide deformation front as defined by Dickinson (1981), and occurred during the relaxation of Laramide compressive stress. The alkalic igneous events of the RMAP are coeval with, but inboard of, the more voluminous calc-alkalic centers of the post-Laramide continental magmatic arc (Fig. 1). In New Mexico, the calc-alkalic activity, represented in part by the Datil-Mogollon volcanic field, occurred from 37 to 30 Ma, just after Laramide deformation but prior to the inception of rifting along the Rio Grande (Chapin and Seager, 1975; Chapin, 1979; Lipman, 1980, 1981; Morgan et al., 1986). Beginning about 30 Ma, extensional tectonism and bimodal volcanism was initiated in the Rio Grande rift, which overprinted the earlier compressional structures and magmatism (Chapin and Seager, 1975; Chamberlin, 1978).

Thus, the LCPB is in a setting that includes features related to convergent tectonics as well as younger rifting. The igneous activity of the LCPB occurred along the margin of the stable craton in New Mexico, which is demarked by the relatively undeformed Pecos slope (Fig. 2), the eastward limit of Laramide deformation in this region (Kelley and Thompson, 1964). An early pulse of magmatism in the LCPB occurred in response to relaxation of Laramide compressive stresses. The onset of rifting along the Rio Grande caused block-faulting and uplift, which resulted in the development of Basin and Range structure and physiography to the west of the Pecos slope. A second pulse of igneous activity, to which the Capitan pluton belongs, occurred during the early stages of rifting.

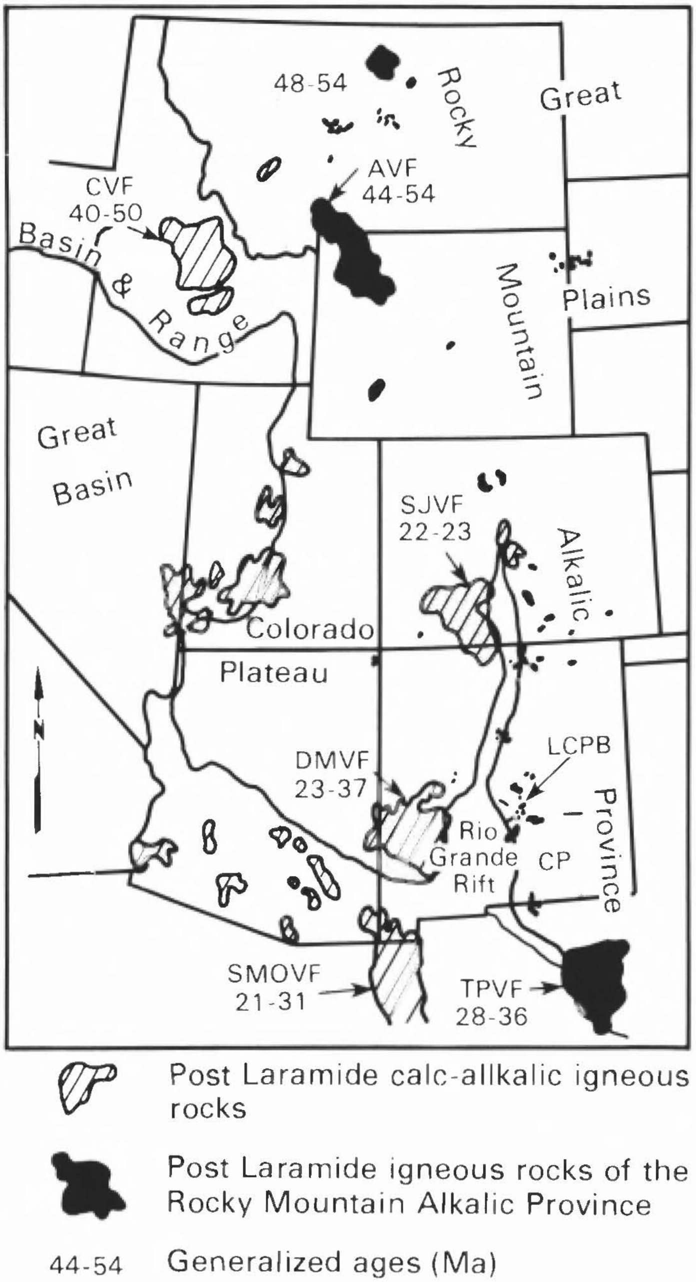

FIGURE 1. Map showing igneous rocks of the Rocky Mountain alkalic province (RMAP), and location of Capitan pluton, New Mexico. Modified from Dickinson (1981) and Stewart and Carlson (1978). AVF—Absaroka volcanic field; CC—Cripple Creek volcanic complex; CP—Capitan pluton; DMVF—Datil-Mogollon volcanic field; LCPB—Lincoln County porphyry belt; SJVF—San Juan volcanic field; SMOVF—Sierra Madre Occidental volcanic field; TPVF—Trans-Pecos volcanic field.

Local structural setting

The igneous rocks of the LCPB are concentrated along and at the intersection of two major structures (Fig. 2), the north-south-trending Pedernal arch and the east-west-trending Capitan lineament (Kelley and Thompson, 1964; Chapin et al., 1978). The Pedernal arch is the remnant of a Pennsylvanian uplift that was eroded and submerged in Permian time (Weber, 1964). Though this structure is largely buried, it can be traced north-south by exposures of Precambrian outcrops from Bent to near Corona (Kelley and Thompson, 1964; Kelley, 1971). This structure roughly controls the location of igneous centers of the LCPB, including the major complexes of Sierra Blanca, and the Jicarilla and Gallinas Mountains.

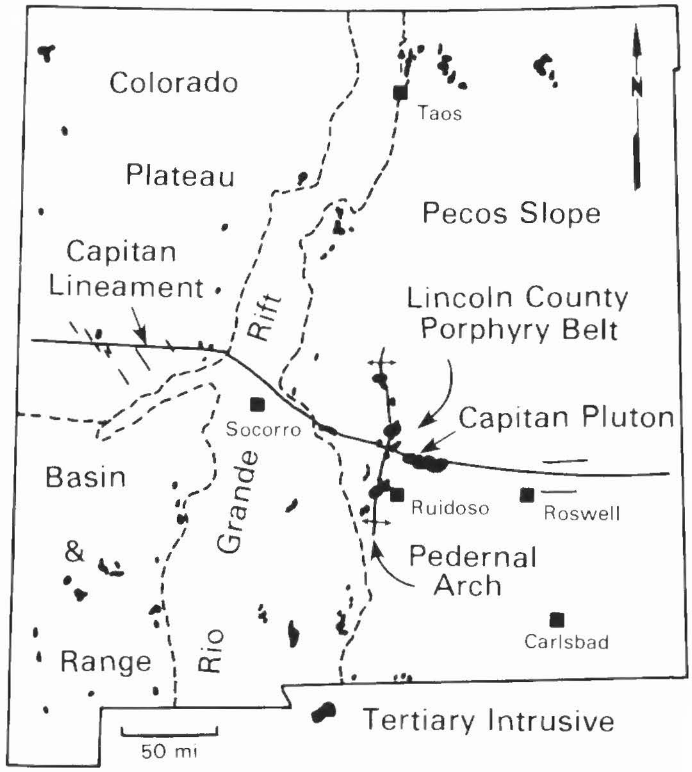

FIGURE 2. Map of New Mexico, showing the Lincoln County porphyry belt and related tectonic features. Modified from New Mexico Geological Society, 1982.

The Capitan lineament, as originally described by Kelley and Thompson (1964), is an alignment of structural and igneous features which includes, from east to west, the Matador arch of west Texas, the diabase dikes near Roswell, the Capitan pluton, the northern truncation of the Carrizozo anticline, the vents of the Quaternary Carrizozo basalt flows, and the composite Jones Camp dike. Chapin et al. (1978) showed the Capitan lineament deflecting northwest at the Rio Grande depression and persisting westward to intersect the southwest-trending Jemez lineament in the vicinity of the Springerville volcanic field of eastern Arizona (Fig. 2). They did not identify which features define the Capitan lineament west of the Rio Grande, however. Allen and Foord (1991b, this volume) propose, based on published ages (approximately 28 Ma) and geochemical data, which are similar for rocks east of the Rio Grande, that the lineament includes the Anchor Canyon/Nitt igneous complex (Weber and Bassett, 1963; Park, 1971) and mafic alkalic dikes near Pie Town (Aldrich et al., 1986).

The Capitan lineament is, therefore, a transcurrent fracture zone of the Rio Grande rift that leaked basaltic and granitic magmas during early stages of rifting, and more recently (<1 Ma) basalts. Differences in stratigraphy and structure north and south of the lineament, however, indicate a long history prior to Tertiary activity. The lineament served as a hinge line that controlled sedimentary depositional styles north and south of it in Paleozoic and Mesozoic times (Kelley and Thompson, 1964). Offset of structural contours on top of Permian strata north and south of the lineament indicate between 15 to 30 km of left lateral motion, or 300 to 490 m of down-to-the-north motion in pre-Tertiary time (Kelley and Thompson, 1964).

PHYSIOGRAPHY

The Capitan pluton is the most prominent feature of the Capitan lineament, with an elongate (35 × 8 km) exposure along the lineament's trend. Uplift and erosion of the pluton have formed an extensive apron surrounding it, such that when viewed from the east, it is seen as a symmetrical triangle (Fig. 3). When viewed from the south or north, the pluton has a relatively flat top that is higher to the east (Fig. 4).

FIGURE 3. Capitan Mountains, viewed from the east. Note triangular cross section due to talus aprons.

FIGURE 5. Eastern end of the Capitan Mountains, showing cliffs and spires developed from erosion of the jointed pluton.

The elevation on the west end of the pluton is approximately 2590 m, whereas Capitan Peak, near the east end, is 3073 m. Deep canyons have been incised into the pluton in its eastern half, resulting in picturesque cliffs and spires (Fig. 5). The topographic relief displayed in this area allows study of 1340 m of vertical exposure into the pluton.

GEOLOGY

Host rocks

Contacts with country rock are poorly exposed due to the extensive apron of talus eroded from the pluton (Fig. 6). On the west end, the pluton intrudes carbonate and minor sandstone lithologies of the Rio Bonito Member of the Permian San Andres Formation. The rest of the pluton intrudes the clastic and minor carbonate and evaporite lithologies of the Permian Yeso Formation. Roof pendants, probably of San Andres Formation, cap the pluton west of Capitan Pass. Carbonate lithologies locally in contact with the intrusion have been altered to calc-silicate and carbonate skarn assemblages and host iron deposits. The largest of these deposits is the Capitan magnetite deposit (now known as the Smokey iron mine), which has an estimated reserve of 1 million tons (Kelley, 1949; Griswold, 1959). This is the largest of numerous iron deposits associated with the Lincoln County porphyries.

Intrusive form

The exact form of the Capitan pluton is difficult to determine, though its large size (280 km^2) demands batholith classification. Tilting of Paleozoic and Mesozoic sedimentary units around the pluton indicates forceful intrusion in Tertiary time. Where contacts are observable at the east and west ends of the pluton, the sedimentary units dip vertically or are overturned (Allen, 1988). Rare exposures along the longitudinal contacts of the pluton display less steeply dipping sedimentary units. The horizontal roof pendants and sill-like tongues of the intrusion into Permian strata on the western end of the pluton may indicate a laccolith form of intrusion (Kelley and Thompson, 1964; Kelley, 1971). A floor to the pluton is not apparent. The pluton's elongate shape, which is oriented along trend with the Capitan lineament, indicates dike-like intrusion along a fault or fracture zone.

FIGURE 4. Capitan Mountains, viewed from the north. Note flat top and wind gap of Capitan Pass in center.

Our observations are equivocal, because evidence exists to support both stock (discordant) and laccolith (concordant) forms. No roof pendants have been found east of Capitan Pass. However, extensive alluvial fans indicate that significant erosion has occurred there, obscuring the initial form of the pluton. Sandstone and limestone clasts and abundant magnetite sand and magnetite-rich cobbles in the alluvial fans from the eastern end are suggestive of a pre-existing cap of Permian strata and iron skarn deposits similar to the Capitan iron deposit (Kelley, 1971). We have observed no evidence of stoping or assimilation of country rock by the pluton, features commonly observed in stocks and batholiths. Other indirect evidence discussed in more detail below, such as the pluton's fine grain-size and granophyric texture, suggests rapid cooling of a shallow magma body, more plausible in a laccolith. We suggest that the pluton be referred to as a batholith, recognizing that its mode of intrusion was forceful injection at a shallow level, which resulted in fine-grained discordant and concordant portions.

Deformation and erosion

The pluton may be bounded on the north and south by faults (Kelley, 1971), though exposure is poor along the flanks due to the alluvial

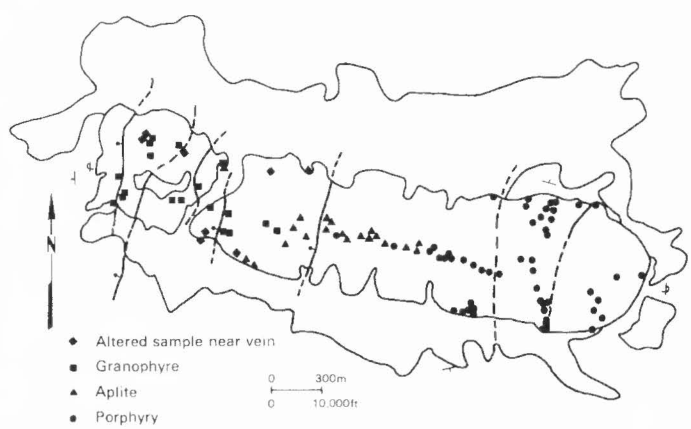

FIGURE 6. Geologic map of the Capitan pluton, showing sample locations.

apron. Kelley and Thompson (1964) estimated that the Capitan fault, which bounds the southwestern side of the pluton, has as much as 396 m of down-to-the-south displacement that decreases in magnitude to the west (Fig. 6). The pluton has also been faulted in places perpendicular to its long axis, resulting in greater uplift, erosion and exposure of the pluton at its east end. The extensive alluvial deposits from the eastern part of the pluton containing sedimentary clasts and magnetite-rich cobbles support the interpretation of erosion of a pre-existing cap. Our petrographic and chemical data add support to this conclusion, showing a progressive zoning deeper into the pluton from west to east. If the pluton intruded a complete sedimentary section from the Permian Yeso Formation to the top of the Tertiary Cub Mountain Formation, as estimated for regions near Capitan by Craddock (1964) and Weber (1964), its total cover could not have exceeded 2.1 to 2.3 km, respectively. Phillips (1990), using fluid inclusion data and stratigraphic reconstruction, estimated the pluton's depth of emplacement to be 1.2 to 1.6 km.

The pluton is extensively jointed. On the ends, two sets of roughly vertical joints are observed, a more dominant east-west set, and a north-south set. Within most of the pluton an east-west joint set is present parallel to its margin. These sets are consistent with strain expected from crystallization pressure in the upper part of a magma chamber (Knapp and Norton, 1981). Dikelets consisting of quartz, albite and titanite are observed along some of the fractures, supporting the hypothesis of late-stage fracturing and magmatic/hydrothermal injection.

Geochronology

Igneous activity in this part of New Mexico spans middle Tertiary to Recent times, but can be divided into three major pulses. The earliest pulse began about 38.2 Ma and continued until about 36.5 Ma, and includes the Jicarilla intrusives (Segerstrom and Ryberg, 1974), and the undersaturated volcanic flows and intrusions of the Sierra Blanca and Black Mountain complexes (Thompson, 1972; Moore et al., 1985; Allen and Foord, 1991b, this volume). The compositional similarities of undersaturated intrusions of the Tecolote Hills and Gallinas Mountains to these rocks suggest they also belong to this early event (Allen, 1991). A second pulse of igneous activity occurred subsequent to the onset of rifting at 30–26.5 Ma, and includes the late silica-saturated phases of Sierra Blanca and several igneous bodies along the Capitan lineament. The Capitan pluton was emplaced at 26.5 ± 1.2 Ma (Allen, 1988), slightly after the mafic dikes along the lineament (Railroad Mountain, Jones Camp and Pie Town dikes at 28 Ma; Aldrich et al., 1986). Textural and compositional similarities of the oversaturated plutons of Carrizo, Lone and Patos Mountains to the Capitan pluton suggest they also belong to this younger pulse (Allen and Foord, 1991b, this volume). Whereas the igneous activity along the Pedernal trend spans both early pulses from 38.2 to 26.5 Ma, Tertiary igneous activity along the Capitan lineament is narrowly restricted from 28 to 26.5 Ma. The Quaternary eruptions of basalt flows near Carrizozo (the Malpais) from vents along the Capitan lineament are among the youngest igneous rocks in New Mexico (Renault, 1970).

Petrology

Samples have been collected from the Capitan pluton at approximately 100 sites to ascertain its textural and mineralogical variations. From reconnaissance field observations, the pluton appears to be a uniform, white, granite aplite (Kelley and Thompson, 1964; Kelley, 1971). However, systematic observation reveals progressive development of a coarser and porphyritic texture from west to east. On the west end, samples contain varying but generally higher percentages of quartz (20–30%) than samples on the east end, and contain no mafic minerals other than iron oxides. Samples from the east end contain varying percentages of quartz (5–25%), feldspar phenocrysts, biotite and richteritic amphibole. Samples from the west end are porous and contain micromiarolites, and appear more altered with pinkish iron staining, suggesting deuteric alteration. Some quartz veins containing fluorite and clinoptilolite (zeolite) (Fig. 6; site #A10), and fractures in the aplite with druses of quartz, feldspar, hematite and titanite (Fig. 6; site #A9) are present in this area. These features are rare in the east end of the pluton and are found only near its margin. Textural and mineralogic variations are gradational, with no evidence for multiple intrusive phases.

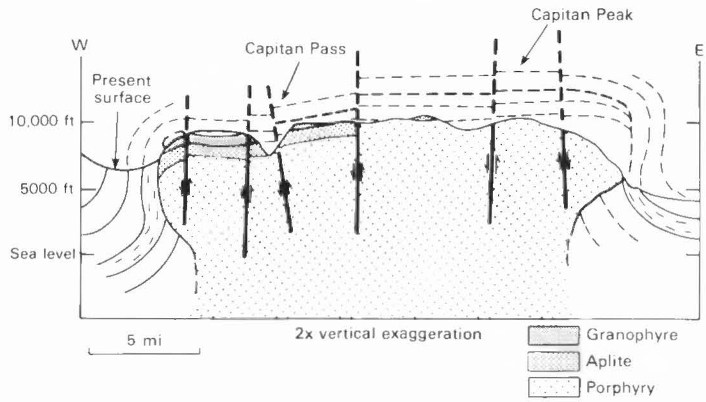

FIGURE 7. Diagrammatic cross section of the Capitan pluton, showing its three textural zones.

The systematic textural and compositional zoning of the pluton are readily observed in thin-section samples. The pluton's vertical exposure and differential uplift allow detailed study of zoning from the roof into the core. The roof zone, preserved on the pluton's west end, consists of a hypersolvus granophyric aplite. Granophyric aplite grades into a core of equigranular to porphyritic amphibole, biotite, subsolvus, alkali feldspar granite. We divide the pluton into three textural zones (Fig. 7)—granophyre, aplite and porphyry—based on petrographic observations, though transitional samples do exist. Chemical data also support this division, showing distinct variations from one texture to another. Due to the fine-grained, granophyric to porphyritic texture, modal classification of Capitan pluton rocks is difficult, and therefore we use the chemical classification scheme of De la Roche et al. (1980). Samples from the Capitan pluton fall within alkali feldspar granite, though porphyritic samples trend toward more normal granite.

Samples collected from the western portion of the pluton, from its western contact zone to just east of Capitan Pass, are fine grained (0.5–2 mm) and have a pronounced micrographic and granophyric texture. Textures range from predominantly micrographic feldspar and quartz (Fig. 8), to a fine-grained allotriomorphic-granular texture with minor intergrowth occupying interstices between quartz and alkali feldspar grains. Occasionally, euhedral K-feldspar crystals are observed with granophyric rims (Fig. 9). Many samples also contain micromiarolites with open space filling by euhedral quartz and albite, and occasionally

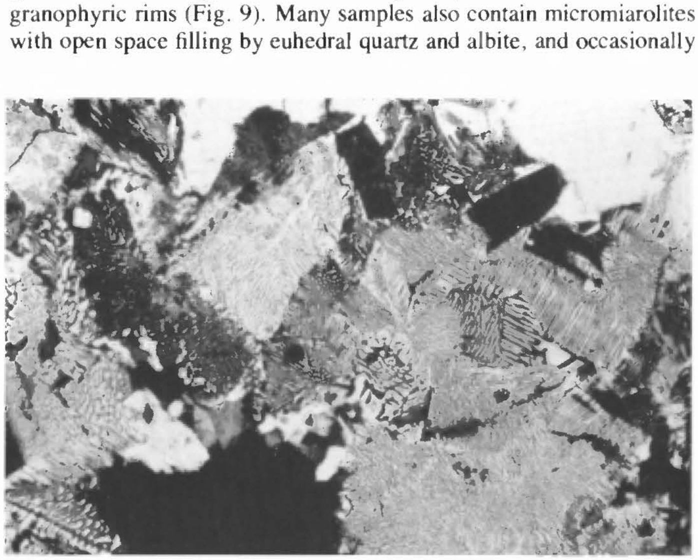

FIGURE 8. Photomicrograph of a sample from the west end of the Capitan pluton, showing micrographic intergrowth of quartz and feldspar.

FIGURE 9. Photomicrograph of a sample from the west end of the Capitan pluton, showing granophyric intergrowth of quartz and alkali-feldspar on alkali-feldspar.

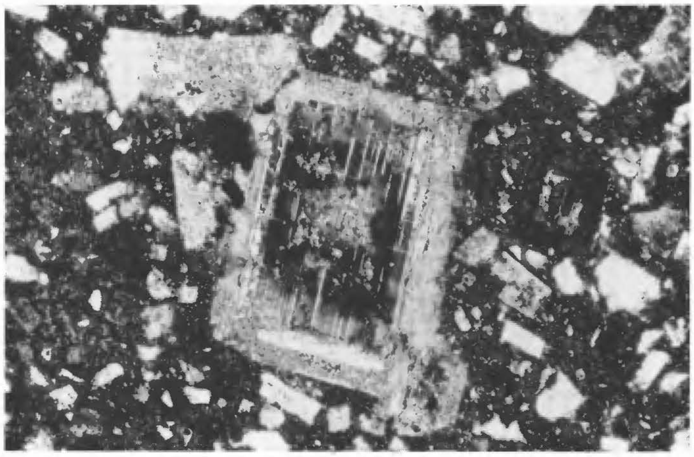

FIGURE 11. Photomicrograph of a porphyritic sample from near the eastern contact of the Capitan pluton, showing plagioclase phenocryst in very fine-grained groundmass. Note seriate broken phenocrysts.

with titanite and fluorite. A dusting of hematite and magnetite is disseminated through these samples. No evidence for pre-existing mafic minerals is observed. Feldspars exhibit varying degrees of alteration from fresh to slight argillic alteration.

Granophyric texture grades into an equigranular textured aplite east of Capitan Pass and is also present in samples from the wind gap of Capitan Pass, where the deeper parts of the pluton have been exposed. Samples display allotriomorphic to hypidiomorphic growth of alkali feldspar and quartz with an average grain size of 1–2 mm (Fig. 10). Feldspars exhibit microperthitic texture. Micromiarolites are rare in these samples. Aggregates of magnetite and richteritic amphibole containing euhedral grains of apatite comprise about 1–2% of the rock. Rarely, blebs of fluorite are present.

Samples from the eastern half of the Capitan Mountains are porphyritic, containing up to 20% phenocrysts of anorthoclase (0.5 to 1 cm) and rare plagioclase (Ab_{90}) up to 0.5 cm in a fine-grained groundmass (Fig. 11). Some plagioclase phenocrysts display zoning, and some phenocrysts of both feldspars may have rims of alkali feldspar. Perthitic rims on anorthoclase occur in less porphyritic samples, which probably formed contemporaneously with groundmass perthite. The porphyritic texture becomes increasingly pronounced toward the east and deeper into the pluton. Microphenocrysts and microaggregates of apatite, zircon, magnetite, titanite, richteritic amphibole and biotite, which crystallized in that order, become more abundant with development of the porphyritic texture (Fig. 12). The overall abundance of accessory minerals rarely exceeds 10%, with magnetite, biotite and amphibole being dominant. Along its eastern contact, the pluton displays a porphyritic-aphanitic texture. Broken and bent (annealed, curvilinear-shaped) phenocrysts of feldspar in a trachytic groundmass indicate rapid crystallization during intrusion (Fig. 13).

GEOCHEMISTRY

Methods

Nineteen samples were collected by the first author for geochemical analysis at the USGS laboratories in Denver and Menlo Park. Major-element oxides were determined using energy-dispersive XRF methods (Johnson and King, 1988). Trace elements and REEs were determined using wavelength-dispersive XRF methods (Taggart et al., 1988), and instrumental neutron-activation analysis (Baedecker and McKown, 1988). Ferrous iron, CO_2, H_2O^+, H_2O^- and F were determined using wet chemical and gravimetric methods (Jackson et al., 1988). Strontium and neodymium isotope analyses were obtained through the University of Colorado, using methods described by Farmer et al. (1991). Eighty samples were collected by the second author and analyzed at the NMBM&MR for major and trace elements. Major elements were determined by XRF on glass discs following the methods of Norrish and Hutton (1969). Trace elements were determined by XRF using pressed-powder briquets. Geochemical data are presented in Table 1. Thirty-seven whole-rock analyses were rejected because of high LOI contents

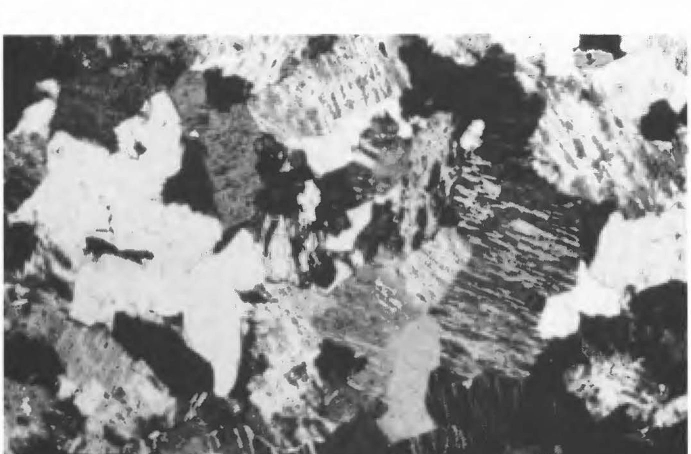

FIGURE 10. Photomicrograph of a sample of the aplite zone of the Capitan pluton, showing allotriomorphic-granular quartz and perthitic alkali-feldspar.

FIGURE 12. Photomicrograph of a porphyritic sample from the east end of the Capitan pluton, showing microaggregate of apatite, magnetite, zircon, titanite, richterite and biotite.

TABLE 1. Geochemical data for rock samples from the Capitan pluton, Lincoln County, New Mexico. Element oxides and LOI are in weight percent; all others are in ppm; Fe_2O_3 is total iron expressed as Fe_2O_3; —, value not determined.

Sample	SiO_2	Al_2O_3	Fe_2O_3	FeO	MgO	CaO	Na_2O	K_2O	TiO_2	P_2O_5	MnO	LOI	Nb	Rb	Sr	Zr	Y	Ba	Th	U	Ta	Co	La	Ce	Nd	Sm	Eu	Gd	Tb	Tm	Yb	Lu
Granophyric Samples																																
A6A	76.0	12.9	0.63	0.01	0.05	0.07	4.55	4.19	0.11	0.02	0.03	0.71	68	134	28	215	74	82.8	27.1	2.73	5.20	0.68	40.6	98.8	44.2	11.5	0.72	12.7	2.21	1.49	9.15	1.25
A11	75.5	13.2	0.78	0.03	0.05	0.04	4.69	4.42	0.15	0.02	0.01	0.59	70	124	28	295	68	39.8	30.1	3.10	5.18	0.13	9.77	119.	15.8	5.37	0.38	7.28	1.49	1.14	7.53	1.05
A12	77.2	13.0	0.53	0.01	0.05	0.07	6.52	1.28	0.12	0.02	0.04	0.41	70	28	32	230	66	56.7	27.1	2.63	5.15	0.18	24.4	70.8	30.7	8.61	0.51	10.9	1.96	1.25	7.18	0.90
A13	74.4	13.0	1.32	0.22	0.13	0.35	4.44	4.92	0.18	0.02	0.02	0.41	52	134	5	270	78	45.9	21.8	3.02	3.81	0.16	46.1	116.	50.1	14.3	0.85	15.1	2.57	1.28	7.68	1.03
A15	74.2	13.3	0.98	0.05	0.10	0.31	4.28	5.18	0.18	0.02	0.01	0.68	68	162	10	330	48	24.0	30.4	3.59	4.09	0.12	43.1	130.	32.4	7.65	0.54	7.44	1.24	0.95	6.35	0.96
A16	73.8	13.3	1.46	0.06	0.05	0.07	4.44	4.85	0.18	0.02	0.01	0.66	66	134	5	325	58	59.0	22.1	4.33	4.67	0.48	2.36	86.9	2.51	1.28	0.23	3.66	1.03	1.23	7.93	1.19
M102	74.1	13.7	1.74	--	0.09	0.14	5.14	4.18	0.20	--	0.02	0.67	68	131	38	362	50	--	32.	6.	--	--	--	--	--	--	--	--	--	--	--	--
M103	75.7	13.3	1.31	--	0.03	0.18	5.63	3.79	0.18	0.01	0.03	0.34	69	128	24	324	66	--	31.	8.	--	--	--	--	--	--	--	--	--	--	--	--
M200	74.1	13.3	1.48	--	0.16	0.21	4.69	5.16	0.20	0.01	0.01	0.41	69	150	24	323	32	--	32.	4.	--	--	--	--	--	--	--	--	--	--	--	--
M223	76.3	13.3	0.79	--	--	0.19	6.94	1.04	0.19	0.01	0.01	0.43	65	25	28	272	58	--	25.	4.	--	--	--	--	--	--	--	--	--	--	--	--
M224	77.2	13.4	1.66	--	--	0.14	4.34	5.22	0.17	0.01	0.02	0.44	67	125	18	267	62	--	27.	5.	--	--	--	--	--	--	--	--	--	--	--	--
M225	75.4	13.5	1.14	--	--	0.15	6.40	2.21	0.18	0.01	0.01	0.39	64	64	39	289	68	--	23.	6.	--	--	--	--	--	--	--	--	--	--	--	--
M228	75.3	13.2	1.20	--	0.01	0.27	4.55	4.94	0.16	0.01	0.01	0.32	70	215	23	275	57	--	25.	3.	--	--	--	--	--	--	--	--	--	--	--	--
M229	74.2	12.8	1.58	--	0.03	0.35	4.07	5.34	0.13	0.01	0.04	0.60	71	226	16	259	72	--	25.	6.	--	--	--	--	--	--	--	--	--	--	--	--
M233	75.5	13.4	1.03	--	--	0.13	5.25	4.29	0.17	0.01	0.01	0.75	69	129	33	306	72	--	27.	3.	--	--	--	--	--	--	--	--	--	--	--	--
M240	73.8	13.8	1.68	--	0.07	0.15	4.92	5.20	0.23	0.01	0.02	0.50	64	157	5	333	51	--	28.	5.	--	--	--	--	--	--	--	--	--	--	--	--
M241	73.4	13.7	1.83	--	0.06	0.15	4.97	5.20	0.23	0.02	0.05	0.22	56	157	11	392	75	--	23.	4.	--	--	--	--	--	--	--	--	--	--	--	--
Aplitic Samples																																
A17	73.0	13.8	1.52	0.21	0.16	0.20	4.60	5.18	0.22	0.02	0.06	0.64	60	142	5	345	78	33.2	27.8	4.31	4.49	0.12	43.6	152.	59.5	16.0	1.07	17.4	2.72	1.48	8.67	1.19
A18	72.7	14.0	1.62	0.11	0.17	0.29	4.57	5.43	0.25	0.02	0.02	0.46	54	148	5	330	80	59.3	25.4	4.20	4.02	0.21	69.7	177.	78.1	19.0	1.26	18.6	2.92	1.44	8.22	1.11
A21	72.7	13.9	1.57	0.20	0.17	0.36	4.73	5.23	0.25	0.02	0.10	0.40	50	138	5	325	74	--	23.1	3.33	--	--	--	--	--	--	--	--	--	--	--	--
A22	72.6	14.0	1.61	0.12	0.19	0.41	4.67	5.19	0.26	0.02	0.03	0.37	52	108	10	355	76	66.2	23.9	3.08	3.81	0.40	67.5	172.	79.6	19.1	1.22	18.3	2.76	1.39	7.99	1.11
A24	72.7	14.0	1.59	0.09	0.18	0.33	4.61	5.29	0.25	0.02	0.06	0.35	58	150	5	400	76	--	31.6	3.09	4.36	0.23	67.0	165.	75.2	17.9	1.18	17.5	2.62	1.31	8.32	1.19
M100	73.4	13.7	1.83	--	0.06	0.15	4.97	5.20	0.23	0.02	0.05	0.22	61	161	15	341	65	--	26.	3.	--	--	--	--	--	--	--	--	--	--	--	--
M101	74.0	13.5	1.69	--	0.08	0.11	4.96	4.88	0.20	0.01	0.02	0.43	65	160	8	304	66	--	21.	6.	--	--	--	--	--	--	--	--	--	--	--	--
M107	73.0	13.8	1.58	--	--	0.50	5.80	5.14	0.22	0.02	0.06	0.59	70	150	23	347	94	--	28.	5.	--	--	--	--	--	--	--	--	--	--	--	--
M221	73.7	14.3	1.20	--	--	0.16	4.91	5.25	0.27	0.02	0.01	0.52	58	143	44	382	22	--	20.	4.	--	--	--	--	--	--	--	--	--	--	--	--
M222	73.0	13.9	1.01	--	0.10	0.22	5.38	4.59	0.26	0.01	0.11	0.38	59	130	49	316	80	--	24.	5.	--	--	--	--	--	--	--	--	--	--	--	--
M242	74.0	13.8	1.77	--	0.02	0.19	5.06	5.00	0.24	0.01	0.01	0.50	64	116	27	352	23	--	27.	6.	--	--	--	--	--	--	--	--	--	--	--	--
M243	72.4	14.0	1.84	--	0.14	0.49	5.01	5.37	0.29	0.05	0.03	0.30	54	119	19	364	80	--	21.	2.	--	--	--	--	--	--	--	--	--	--	--	--
M246	73.1	14.0	1.80	--	0.05	0.41	4.95	5.23	0.26	0.01	0.04	0.35	54	165	14	315	75	--	21.	2.	--	--	--	--	--	--	--	--	--	--	--	--
M256	73.5	13.8	1.71	--	0.09	0.40	5.15	5.24	0.27	0.01	0.08	0.44	54	165	7	370	78	--	24.	4.	--	--	--	--	--	--	--	--	--	--	--	--
M257	72.6	14.2	1.89	--	0.11	0.51	5.10	5.39	0.28	0.02	0.05	0.40	52	142	16	316	81	--	23.	3.	--	--	--	--	--	--	--	--	--	--	--	--
M258	73.3	14.0	1.82	--	0.10	0.42	5.07	5.21	0.27	0.01	0.04	0.68	57	158	5	368	75	--	23.	3.	--	--	--	--	--	--	--	--	--	--	--	--
Porphyritic Samples																																
A5	69.7	14.7	2.34	0.26	0.41	0.64	3.99	5.63	0.38	0.06	0.01	1.29	38	88	130	425	46	827.	20.4	4.99	2.75	1.15	54.2	105.	55.6	12.6	2.26	11.4	1.54	0.86	5.35	0.79
A26	69.7	14.6	2.28	0.47	0.38	0.92	3.79	6.06	0.40	0.07	0.04	0.75	38	138	145	465	68	737.	19.0	3.56	2.54	0.86	124.	262.	102.	18.3	2.61	15.7	2.08	1.02	6.14	0.89
A28	69.7	15.1	2.04	0.28	0.34	0.98	3.95	6.00	0.42	0.07	0.01	0.93	34	110	156	405	52	943.	17.7	3.71	2.38	0.77	126.	266.	99.9	17.2	2.87	13.7	1.86	0.92	5.44	0.78
A29	69.6	15.1	2.02	0.20	0.33	0.86	4.09	5.76	0.44	0.07	0.05	1.47	34	112	74	430	54	951.	18.2	3.11	2.04	1.03	152.	305.	123.	19.9	3.19	14.2	2.00	0.96	5.70	0.83
A34	70.1	15.1	1.89	0.36	0.38	0.93	4.30	5.80	0.40	0.07	0.06	1.71	36	108	68	420	60	580.	18.4	2.92	2.66	0.80	130.	277.	108.	20.1	2.66	15.6	2.20	1.03	6.29	0.89
A35	70.0	14.9	2.00	0.14	0.34	0.89	4.17	5.84	0.42	0.07	0.06	0.63	32	114	62	410	52	760.	17.8	3.16	2.38	0.90	127.	269.	101.	17.0	2.84	13.8	1.85	0.90	5.49	0.82
A50	70.7	15.6	0.76	0.51	0.28	0.83	4.67	5.35	0.44	0.03	0.01	0.91	34	116	180	465	54	769.	17.8	3.19	2.52	0.52	59.9	192.	100.	18.7	2.79	13.9	1.91	0.94	5.58	0.80
A54	70.1	14.9	2.03	0.51	0.39	0.89	4.19	5.64	0.42	0.09	0.06	0.65	32	108	66	405	52	926.	18.6	3.30	2.49	1.12	125.	268.	103.	18.0	2.89	14.0	1.86	0.96	5.63	0.82
M211	69.9	14.9	2.35	--	0.22	0.98	4.43	5.59	0.44	0.06	0.07	0.69	34	120	78	476	47	--	16.	3.	--	--	--	--	--	--	--	--	--	--	--	--
M214	70.5	14.8	2.40	--	0.37	1.05	4.23	5.68	0.42	0.06	0.09	1.13	33	129	84	463	50	--	18.	3.	--	--	--	--	--	--	--	--	--	--	--	--
M245	71.8	13.8	1.77	--	0.09	0.41	4.92	5.27	0.27	0.02	0.05	0.42	54	149	24	390	79	--	22.	3.	--	--	--	--	--	--	--	--	--	--	--	--
M247	72.9	14.1	1.98	--	0.06	0.50	4.87	5.34	0.27	0.02	0.04	0.35	52	148	16	375	73	--	24.	3.	--	--	--	--	--	--	--	--	--	--	--	--
M248	70.9	14.4	1.90	--	0.06	0.52	5.04	5.34	0.29	0.02	0.08	0.74	47	167	10	229	73	--	19.	2.	--	--	--	--	--	--	--	--	--	--	--	--
M249	73.2	14.2	1.94	--	0.04	0.49	4.90	5.48	0.27	0.01	0.06	0.35	50	141	24	356	70	--	18.	2.	--	--	--	--	--	--	--	--	--	--	--	--
M250	72.9	14.1	1.90	--	0.14	0.52	4.62	5.35	0.26	0.02	0.05	0.94	55	131	37	367	76	--	21.	4.	--	--	--	--	--	--	--	--	--	--	--	--
M251	72.4	14.1	1.90	--	0.11	0.53	4.51	5.42	0.28	0.01	0.03	0.79	50	144	28	368	69	--	25.	4.	--	--	--	--	--	--	--	--	--	--	--	--
M253	72.2	13.9	2.00	--	0.08	0.51	4.73	5.40	0.26	0.01	0.05	0.41	53	141	32	369	79	--	23.	6.	--	--	--	--	--	--	--	--	--	--	--	--
M254	72.9	14.2	1.81	--	0.12	0.50	4.80	5.44	0.26	0.02	0.05	0.63	54	156	22	358	78	--	22.	4.	--	--	--	--	--	--	--	--	--	--	--	--
M255	72.6	13.7	1.86	--	0.06	0.47	4.81	5.36	0.26	0.02	0.06	0.63	56	179	13	364	78	--	27.	4.	--	--	--	--	--	--	--	--	--	--	--	--
M259	71.3	13.6	1.88	--	0.16	0.53	4.88	5.31	0.26	0.02	0.04	0.39	55	138	9	364	82	--	24.	3.	--	--	--	--	--	--	--	--	--	--	--	--
M285	70.5	14.8	2.35	--	0.32	0.50	3.99	6.04	0.38	0.05	0.03	1.22	--	--	--	--	--	--	--	--	--	--	--	--	--	--	--	--	--	--	--	--
M299	73.4	14.5	1.04	--	0.04	0.48	5.48	4.78	0.28	0.01	0.01	0.57	--	--	--	--	--	--	--	--	--	--	--	--	--	--	--	--	--	--	--	--
M300	69.2	15.3	2.10	--	0.51	0.84	3.99	6.81	0.39	0.07	0.02	0.90	--	--	--	--	--	--	--	--	--	--	--	--	--	--	--	--	--	--	--	--
M301	72.4	14.5	1.87	--	0.13	0.53	4.57	5.31	0.28	0.04	0.03	0.65	--	--	--	--	--	--	--	--	--	--	--	--	--	--	--	--	--	--	--	--
M302	71.1	15.3	2.18	--	0.38	0.95	4.53	5.63	0.43	0.07	0.10	0.53	--	--	--	--	--	--	--	--	--	--	--	--	--	--	--	--	--	--	--	--
M303	70.5	15.1	2.25	--	0.37	0.96	4.40	5.63	0.42	0.09	0.08	0.78	--	--	--	--	--	--	--	--	--	--	--	--	--	--	--	--	--	--	--	--
M304	70.6	14.8	2.13	--	0.50	0.87	4.44	5.51	0.41	0.07	0.06	0.47	--	--	--	--	--	--	--	--	--	--	--	--	--	--	--	--	--	--	--	--
M305	72.3	14.8	1.84	--	0.27	0.57	4.96	5.18	0.31	0.05	0.03	0.60	--	--	--	--	--	--	--	--	--	--	--	--	--	--	--	--	--	--	--	--
M307	71.1	15.2	2.15	--	0.43	1.01	4.69	5.49	0.43	0.08	0.02	0.58	--	--	--	--	--	--	--	--	--	--	--	--	--	--	--	--	--	--	--	--

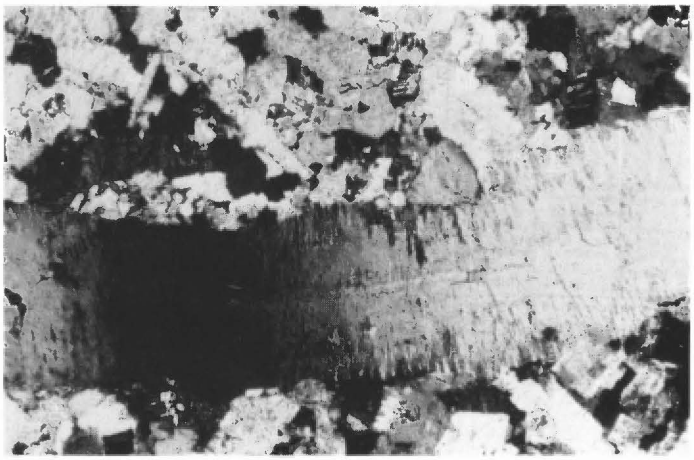

FIGURE 13. Photomicrograph of a porphyritic sample from near the eastern contact of the Capitan pluton, showing "bent" alkali-feldspar phenocryst in fine-grained groundmass.

due to alteration or weathering. Oxygen isotope data were obtained from Phillips (1990).

Classification and normative mineralogy

Average major element contents and CIPW norms for samples from the three textural zones of the Capitan pluton are presented in Table 2. The Capitan pluton can be classified as alkali-feldspar granite using the nomenclature of De la Roche et al. (1980), though some variation is observed. CIPW norms show that porphyritic samples are less quartz-normative and more hypersthene-, anorthite- and magnetite-normative than roof-zone granophyric samples. On average, both granophyric and porphyritic samples are slightly corundum-normative, whereas aplitic samples are not.

TABLE 2. Average major element oxide contents and CIPW norms for the three textural zones of the Capitan pluton, New Mexico. All values are in weight percent; Fe_2O_3 is total iron expressed as Fe_2O_3; diff. index is sum of normative quartz, alkali-feldspar and feldspathoids.

	Granophyre (mean/dev.) (n=17)	Aplite (mean/dev.) (n=16)	Porphyry (mean/dev.) (n=29)
SiO_2	75.0/1.2	73.1/0.5	71.2/1.3
Al_2O_3	13.3/0.3	13.9/0.2	14.6/0.5
Fe_2O_3	1.28/0.40	1.61/0.23	1.97/0.34
FeO	0.06/0.07 n=6	0.15/0.05 n=5	0.34/0.13 n=8
MgO	0.07/0.04 n=14	0.12/0.05 n=13	0.25/0.15
CaO	0.17/0.09	0.33/0.13	0.71/0.21
Na_2O	5.04/0.80	4.97/0.32	4.52/0.39
K_2O	4.24/1.32	5.17/0.21	5.57/0.36
TiO_2	0.18/0.03	0.25/0.02	0.35/0.07
P_2O_5	0.012/0.005	0.018/0.01	0.049/0.03
H_2O+	0.29/0.07 n=6	0.26/0.06 n=5	0.42/0.14 n=8
F	0.04/0.04 n=6	0.04/0.02 n=5	0.03/0.01 n=8
MnO	0.024/0.012	0.047/0.029	0.047/0.024
LOI	0.49/0.16	0.76/0.33	0.76/0.33
		CIPW normative minerals (Fe^{2+}/Fe total = 0.7)	
quartz	29.0	23.5	21.5
corundum	0.25	--	0.03
orthoclase	25.3	30.7	33.2
albite	43.0	42.3	38.6
anorthite	0.48	0.35	3.04
diopside	--	0.77	--
hypersthene	1.03	1.04	1.97
magnetite	0.54	0.70	0.86
ilmenite	0.34	0.48	0.67
apatite	0.03	0.04	0.12
fluorite	0.08	0.08	0.05
Diff. index	97.2	96.5	93.3

Major element trends

Using the definition proposed by Shand (1922), a rock is alkalic if it has total alkalis in excess of that necessary to combine with silica or alumina to form feldspar. Thus, a syenite or granite may have an alkalic affinity if it contains a feldspathoid or an alkali-rich amphibole or pyroxene. The presence of richterite and almost no anorthite in the norm in the Capitan samples indicates an alkalic affinity. Silica and total-alkali contents of the pluton range from 69.6% and 10%, respectively, in porphyritic samples to 77.2% and 8%, respectively, in granophyric samples. On an Irvine and Baragar (1971) silica-vs.-alkali discrimination diagram, all of the Capitan samples are subalkalic, though porphyritic samples lie near the alkalic boundary (Fig. 14). Based on the ACF ternary diagram of White and Chappell (1977), the Capitan samples are I-type except for roof-zone, deuterically altered samples, which plot near the "A" apex and are indeterminate, or plot in the S-type field (Fig. 15).

The major element oxides of Al, Ca, Mg, Fe, Ti and P (not shown) all have negative correlation with silica, and display progressive depletion from east to west (Fig. 16). These trends are consistent with trends expected from fractionation of amphibole, plagioclase, iron and titanium oxide minerals, and apatite, suggested by microaggregates of these minerals in porphyritic samples from deeper in the pluton. Altered samples collected near mineralized veins show elevated TiO_2 contents, which correlate with the presence of euhedral titanite in micromiarolites.

The oxides of Na and K show irregular trends with respect to the other oxides (Fig. 16). Generally, K_2O displays slight depletion with increasing silica content, but samples with abundant micromiarolites and samples taken near mineralized veins exhibit pronounced depletion. On the other hand, Na_2O shows regular enrichment correlative with increasing silica content. Altered samples depleted in K_2O display the greatest Na_2O enrichment, suggesting higher activity of Na_2O in late-stage melt and/or magmatic/hydrothermal fluid. Albite is present as euhedral crystals in micromiarolites, and data from study of fluid inclusions in quartz from veins indicate the presence of a late-stage aqueous

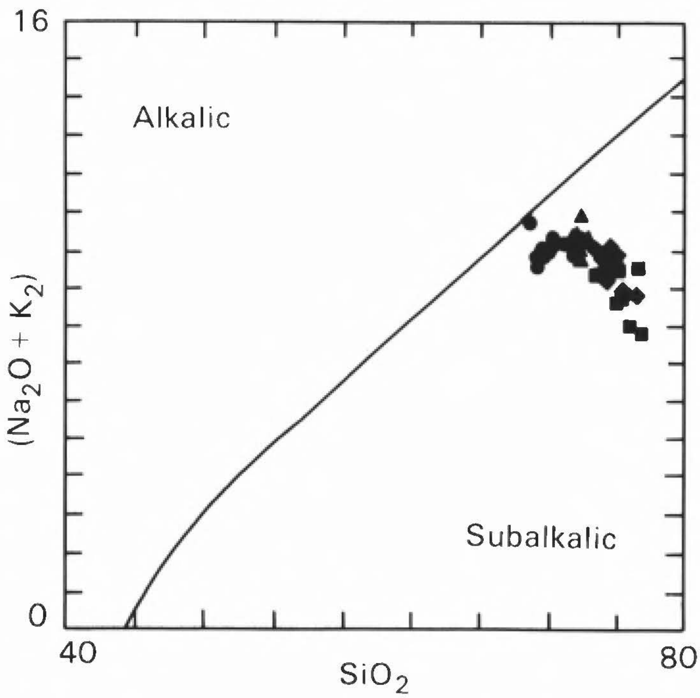

FIGURE 14. Plot showing samples from the Capitan pluton on an Irvine and Baragar (1971) alkali versus silica discrimination diagram.

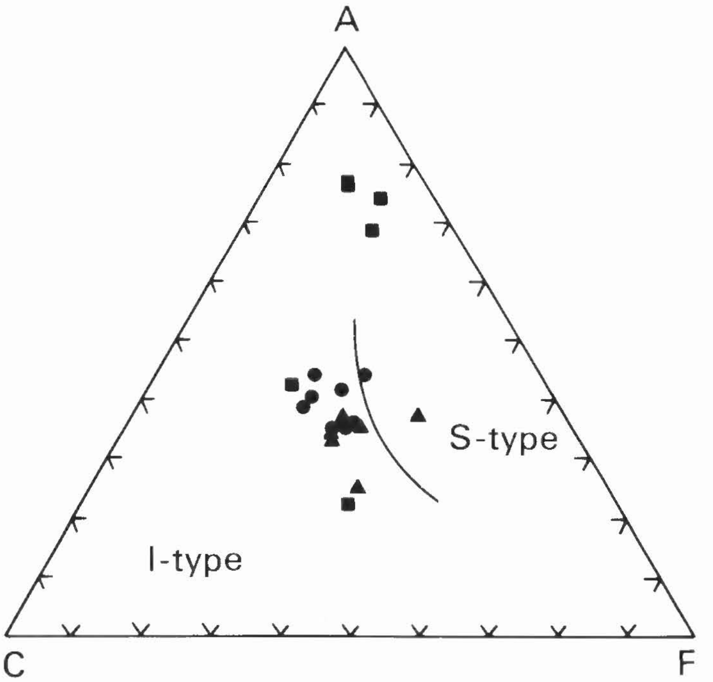

FIGURE 15. Plot showing samples from the Capitan pluton on a White and Chappell (1977) ACF ternary discrimination diagram. A = Na_2O; C = CaO; F = FeO + 0.889 × Fe_2O_3; all in weight percent.

fluid of extremely high salinity with an average Na/K ratio of about four (Phillips et al., 1990).

Granophyric textures have been interpreted to indicate quenching of a eutectic composition in the granite system (Barker, 1970; Swanson, 1976; Fenn, 1979). Capitan pluton granophyre samples plot close to a eutectic composition at 2 kb pressure (Fig. 17), supporting the hypothesis of quenching of a shallow, equilibrated granite system for the Capitan roof-zone. This pressure, however, seems unreasonably high when compared to the stratigraphic reconstruction of possible sedimentary cover. This discrepancy may be explained by Fenn (1986), who showed that the intergrowth of quartz and alkali feldspar can also result from nonequilibrium crystallization controlled by boundary-layer kinetics. This occurs when feldspar growth rate exceeds the rate of diffusion of chemical components from the melt to the site of crystallization, which leaves the boundary layer near feldspar saturated with respect to silica. The silica enrichment in the boundary layer allows the simultaneous growth of quartz and feldspar, even though the bulk composition of the melt should only allow feldspar growth. Observed textures in the Capitan samples support both eutectic and non-eutectic growth. Samples composed predominantly of micrographic intergrowth probably represent eutectic crystallization, whereas aplitic samples with granophyre developed on euhedral feldspar in crystallographic continuity probably represent kinetically controlled growth. In either case, rapid crystallization is indicated.

Trace element trends

The trace elements Ba, Co, Ni, Sr, Zr and LREE display negative correlation with silica (Fig. 18). Porphyritic samples containing the highest quantities of these elements also contain microaggregates of accessory minerals. Depletion of these elements in aplitic and granophyric samples is compatible with fractionation of alkali-feldspar (Ba), amphibole and magnetite (Co, Ni), plagioclase (Sr), apatite (Sr, LREE) and zircon (Zr) from a core-composition melt. Tantalum, Nb, Th, Y and HREE appear incompatible, displaying positive correlation with silica content and enrichment in the roof zone (Fig. 18).

Ratios of incompatible elements may be useful in obtaining information on source materials from which magmas are derived, because these ratios should not change through fractionation (Arth, 1976). The two most incompatible elements for the Capitan pluton are Ta and Nb, which exhibit high covariance ($r = 0.97$) and a Nb/Ta ratio of 13.5. This covariance is consistent with the hypothesis that zoning of the Capitan pluton is not the result of melting of different sources.

Rare-earth-element patterns

Rare-earth-element (REE) patterns provide information concerning phases important in fractionation processes of igneous/hydrothermal systems, and also help constrain the composition of melting sources for magmas. Rare-earth-element patterns plotted for 17 samples representative of the three textural zones of the Capitan pluton (Fig. 19) are mostly subparallel, LREE-enriched and have negative Eu anomalies. Systematic depletion of LREE and enrichment of HREE (La/Lu from 10 to 4.6), and more negative Eu anomalies (Eu/Eu* from 0.43 to 0.16), are observed for samples from the core to the roof of the pluton. Due to the simple composition of this granite system, the variation in REE (except Eu) abundances probably is controlled by accessory minerals with high distribution coefficients for the REE (Hanson, 1980; Miller and Mittlefehldt, 1982; Mahood and Hildreth, 1983). The subparallel, flattening patterns with increasingly negative Eu anomalies are consistent with fractionation of LREE-rich phases apatite, titanite, zircon and feldspar to produce the observed zonation of the pluton.

Granophyric samples containing micromiarolites display non-parallel patterns with severe depletion of LREE except Ce, which may indicate crystallization from an aqueous fluid (Hanson, 1980), and/or mobility and removal of the 3+ cations from the melt into a vapor phase. Cerium, with a 4+ valence under oxidation, appears to be immobile. Quartz-adularia veins in the roof and margin zones of the pluton are known to contain REE- and thorium-bearing minerals titanite, allanite and thorite (Griswold, 1959; McLemore, 1983; Tuftin, 1984; McLemore et al., 1988a, b; Willis et al., 1989; Phillips and McLemore, 1989; Phillips et al., 1990). Fluid-inclusion and stable-isotope studies indicate that these minerals were deposited from high-temperature and high-salinity, magmatic/hydrothermal solutions (Willis et al., 1989; Phillips, 1990; Phillips et al., 1990). Daughter minerals observed in the studies of fluid inclusions include halite, sylvite, anhydrite, barite, hematite, magnetite, titanite, an unknown carbonate mineral, and complex salts of Fe, Mg, Ca, Mn and Zn (Phillips, 1990). The iron-bearing minerals indicate this fluid may also have been important in the genesis of the iron skarn deposits.

All igneous rocks of the LCPB display LREE-enriched patterns (Allen and Foord, 1991a), implying either melting of a LREE-enriched source or melting of a source with garnet in the residue (Hanson, 1978, 1980). Mafic and felsic rocks of the Capitan lineament show similar abundances of REE, which makes their relationship via fractional crystallization unlikely (Allen and Foord, 1991b, this volume). Whereas the undersaturated rocks of the LCPB display REE patterns generally lacking negative Eu anomalies, the silica-oversaturated rocks of the LCPB all display straight patterns with significant negative Eu anomalies. This is true of the Capitan granite, the alkali-feldspar granite of the Sierra Blanca complex, and the quartz syenites of Carrizo Mountain, Lone Mountain and the Jones dike. Development of negative Eu anomalies in magmas may be attributed to fractionation of feldspar during crystallization and/or may be a product of partial melting of a Eu-depleted source or one that has plagioclase left in the restite. The pronounced depletion of Eu in the oversaturated plutons of the LCPB indicates that feldspar fractionation is at least somewhat important in the development of their compositional zoning. However, negative Eu anomalies and straight LREE-enriched patterns for the least-differentiated Capitan samples and other silica-oversaturated plutons of the LCPB, are consistent with melting of a plagioclase-bearing source. The LREE-enriched patterns for silica-oversaturated plutons of the LCPB, including the Capitan pluton, are consistent with their derivation from lower crust possibly containing garnet. However, Allen and Foord (1991a) believe, based on REE and isotopic data for both alkalic mafic and silica-oversaturated rocks of the LCPB, that LREE enrichment may be caused by metasomatism of both mantle and lower crust.

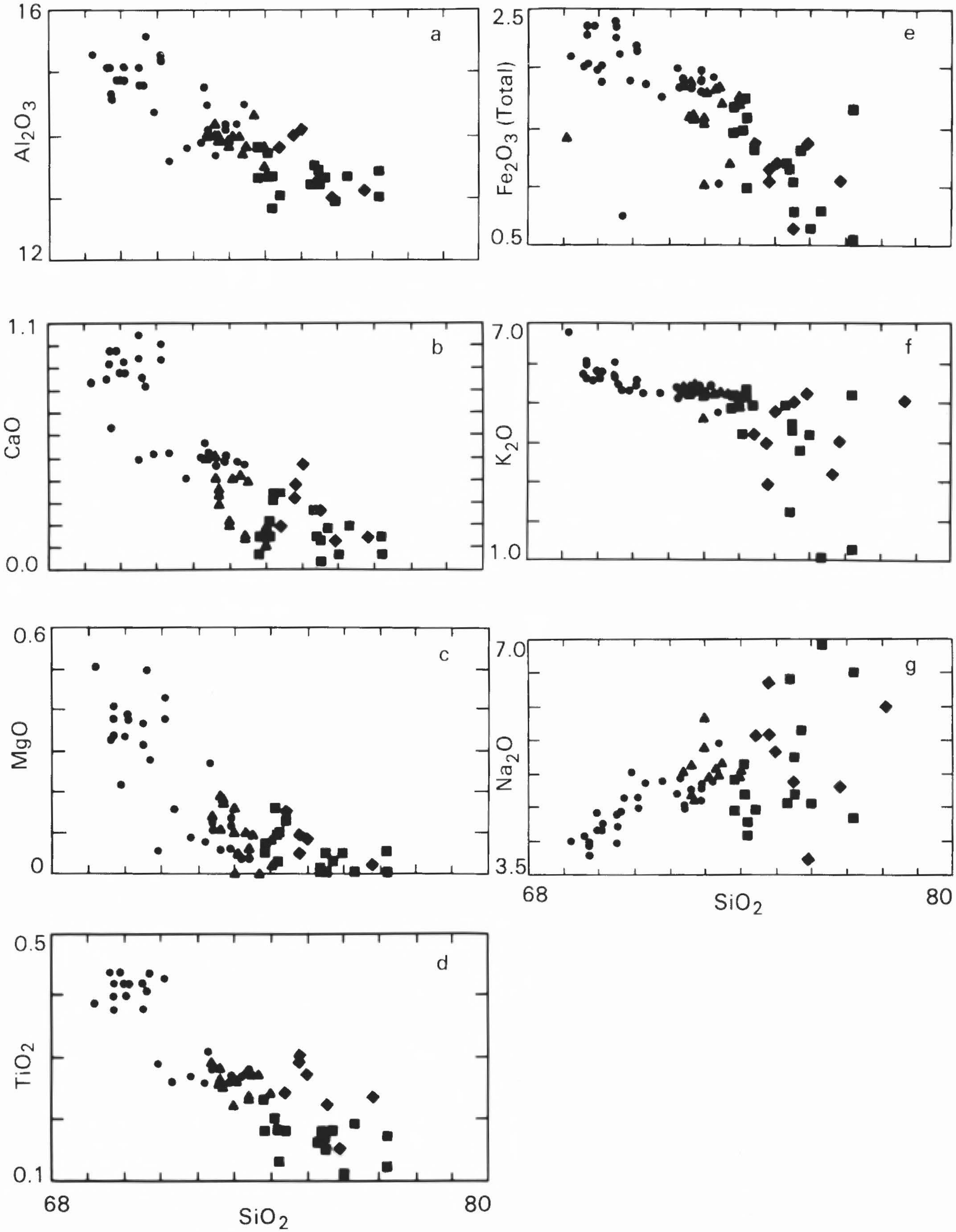

FIGURE 16. Major element (Harker) variation diagrams for samples from the Capitan pluton.

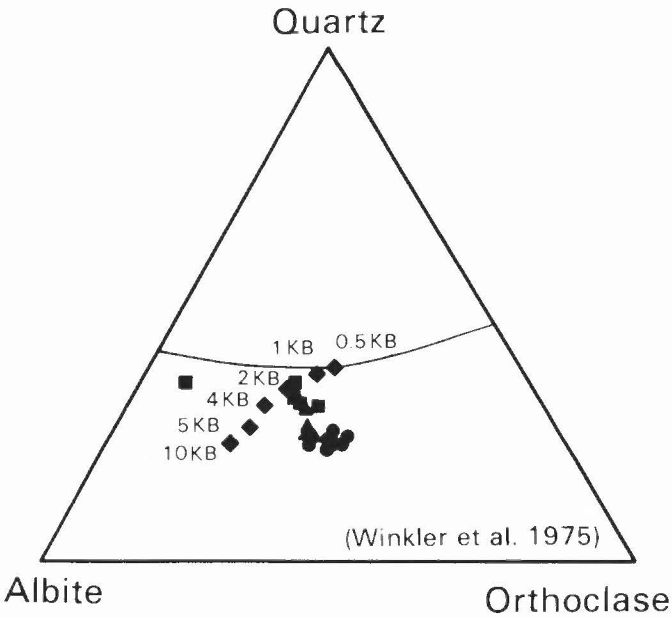

FIGURE 17. Plot showing samples from the Capitan pluton on a Q-Ab-Or ternary diagram with eutectic points at various confining pressures for $P_{H2O} = P_{total}$ conditions, from Winkler et al. (1975).

Isotopes

Measurements of heavy radiogenic isotopes are useful in further constraining magma sources. Strontium and neodymium isotope compositions were determined on one sample of the Capitan granite (Fig. 6, #A35). It contains 127 ppm Rb, 51.8 ppm Sr, a measured 87/86 Sr ratio of 0.71068, and an initial 87/86 Sr ratio of 0.70801. The sample also contained 17.0 ppm Sm, 101 ppm Nd, a measured 143/144 Nd ratio of 0.512364, an initial 143/144 Nd ratio of 0.512346 and an epsilon Nd relative to CHUR (DePaolo and Wasserburg, 1976) of –5.3. These data support the interpretation from the REE data that the Capitan pluton was probably derived from the lower crust.

Oxygen isotope values obtained on whole rock samples from the Capitan pluton range from $\delta^{18}O = +7.64$ to $+9.22$ per mil. There is no systematic variation from roof zone to core. These values are consistent with derivation of the Capitan pluton magma from an igneous or I-type source in the lower crust (O'Neil et al., 1977).

GENETIC MODEL

Tectonic development

The Capitan pluton was generated during the later of two periods of igneous activity in the LCPB. The first period of activity was probably confined to 38.2 to 36.5 Ma and includes the mafic alkalic complexes (Sierra Blanca, Tecolote Hills, Jicarilla Mountains and Gallinas Mountains) distributed along the north-trending Pedernal arch (Allen and Foord, 1991, this volume). This period corresponds to the waning stages of Laramide compressional tectonics due to subduction beneath southwestern North America. During this time, voluminous calc-alkalic magmas reached the surface to form the extensive lava flows, ash sheets and caldera complexes of western New Mexico. The paleo-stress model of Price et al. (1987) for southeastern New Mexico indicates that the Ruidoso region was under some northeast-directed compression during this time, which inhibited opening of the east-west fractures along the Capitan lineament.

A change from northeast-directed compression to east-west extension during the onset of rifting caused opening of new fracture systems and was accompanied by a second period of igneous activity concentrated along the east-west Capitan lineament in the Ruidoso region. Igneous activity along the Capitan lineament was restricted to a narrow time span from 28 to 26.5 Ma, and includes mafic alkalic rocks, such as

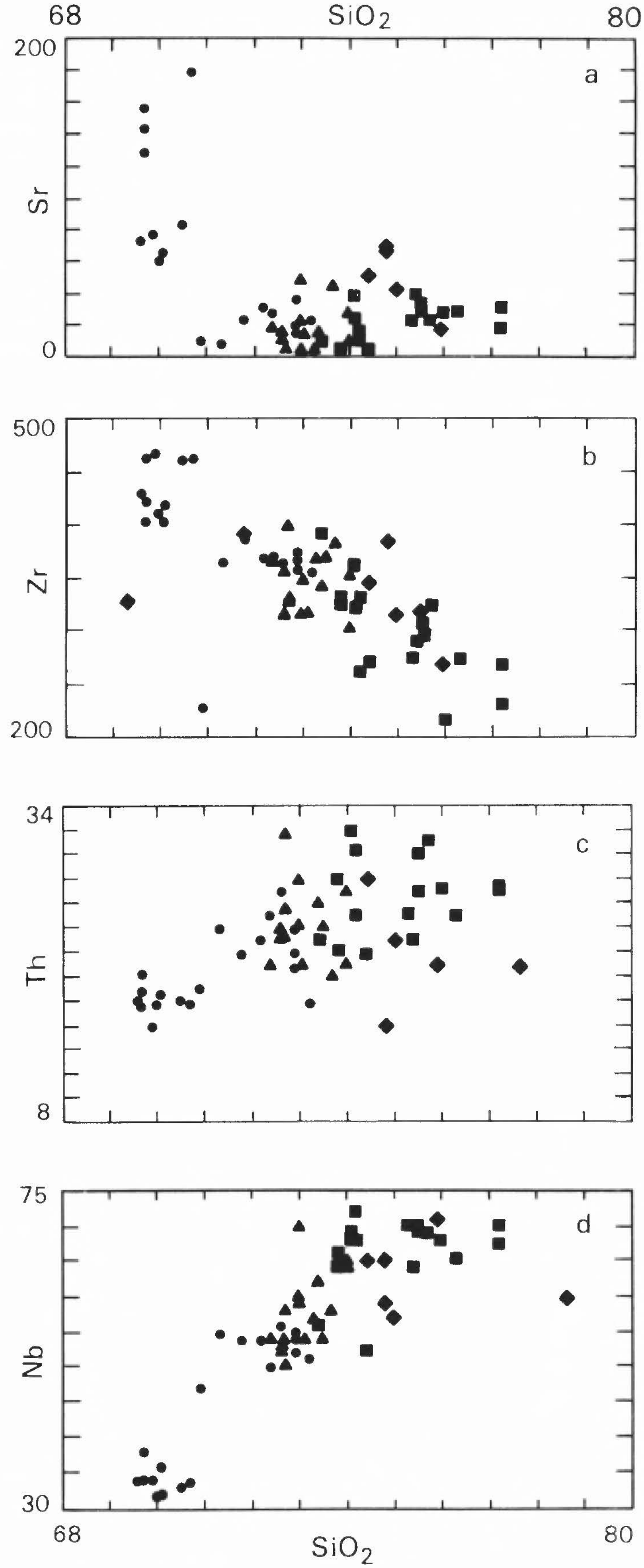

FIGURE 18. Trace element variation diagrams for samples from the Capitan pluton.

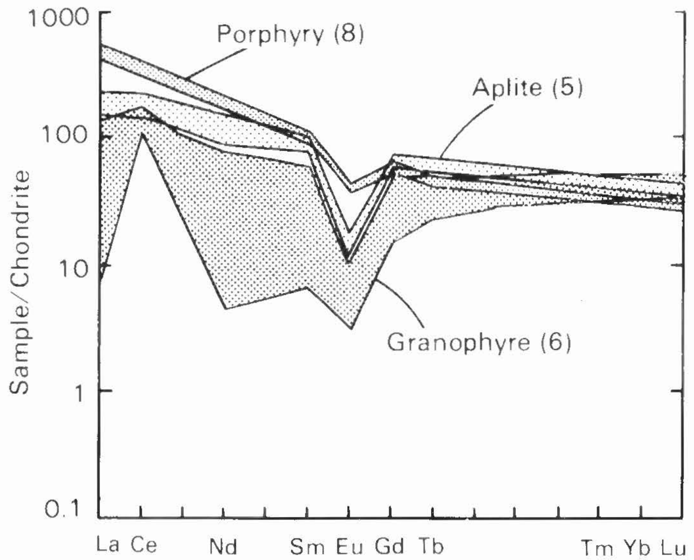

FIGURE 19. Chondrite-normalized REE patterns for samples from the Capitan pluton.

the Railroad Mountain, Jones Camp (margin), and Pie Town dikes, as well as felsic, silica-oversaturated rocks, such as the Capitan, Carrizo Mountain, Lone Mountain and Anchor Canyon/Nitt plutons. This widespread rift-related activity indicates the large areal extent of partial melting beyond the axis of the rift. It is interesting to note that the siliceous igneous rocks of the Capitan lineament are concentrated near the present-day axial basins of the rift, whereas mafic-alkalic compositions occur on either side. This may indicate tapping of shallow versus deep sources, or more intensive melting along the rift axis which incorporated a crustal source.

A more detailed discussion of the causes of melting for the two igneous periods that generated the LCPB is presented by Allen and Foord (1991b, this volume). Fractionation, and some crustal contamination, of mantle-derived mafic-alkalic magmas is believed to have generated the older igneous complexes. Generation of the mafic-alkalic and siliceous magmas along the Capitan lineament during the second igneous period suggests an intimate melting relationship between the magma types. Production of the felsic, silica-oversaturated magmas of the Capitan lineament was caused by the partial melting of lower crust, either through introduction of mantle-derived mafic magmas, or by decompression and/or volatile fluxing beneath this region in response to rifting. The latter model is more consistent with the similar LREE-enrichment displayed by all of the rocks of the LCPB and their diverse isotope systematics.

Discussion of zoning in silicic magmas

The history of the processes that operated on the Capitan pluton magma after its generation and before its emplacement and rapid crystallization at a shallow level is uncertain, but is of primary importance in understanding the pluton as it now exists. Substantial fractionation of the magma is indicated by its varied composition and systematic zoning. The presence of euhedral phenocrysts and high-temperature-mineral microaggregates in the core of the Capitan pluton suggests that fractionation of certain minerals led to its zoning. Geochemical data are also consistent with the fractionation of feldspar, magnetite, amphibole, apatite, titanite and zircon to produce the zoning. The mechanism and timing of compositional zoning in the Capitan pluton is, however, problematic due to its apparent rapid crystallization.

Segregation of liquid and crystals through settling is often called on to explain the zoning observed in igneous rocks. In viscous granite magmas in high-level chambers, this process is probably insignificant considering the relatively short crystallization time (approx. 32,000 yr) of a granite magma body of the Capitan pluton's dimensions (Knapp and Norton, 1981). Assuming an alkali-feldspar-granite liquid with no crystals, $T_{initial} = 650°C$, 3% dissolved water, and $P_{total} = 2kb$, albite crystals 2 mm and 2 cm in diameter would settle 20 cm and 20 m, respectively, in 50,000 yr (McBirney, 1984; Geist et al., 1985). In the extreme case of 500,000 yr, these same crystals could only settle 20 m and 200 m, respectively. For the same conditions, magnetite crystals 0.2 mm and 2 mm in diameter would settle only 4 cm and 4 m, respectively, in 50,000 yr and 40 cm and 40 m, respectively, in 500,000 yr. These settling rates would decrease with the increase in magma viscosity due to the onset of crystallization. Addition of volatiles, such as fluorine, to the system would reduce viscosity, but not sufficiently so. Considering its silicic composition, fine-grained nature and apparent rapid crystallization, physical segregation of components with specific gravities near that of granite melt, such as feldspar, seems unlikely. Even the microaggregates of dense accessory minerals observed in the porphyritic samples are of such small size that there would have been insufficient time for any appreciable settling.

Other mechanisms, such as chemical diffusion or flow differentiation, must be considered for development of the zoning in the Capitan pluton. Normal diffusion rates in granitic melts are too slow for such a wide range in compositions over the large vertical distance in the pluton (Shaw, 1974). Hildreth (1979) proposed a mechanism of thermogravitational diffusion to explain the zoning of the Bishop Tuff magma chamber (similar in magnitude to the Capitan pluton), whereby chemical components are more efficiently segregated through complex interactions of convection, diffusion, complexing and wall-rock interactions. Several workers have disputed this interpretation on the grounds of the sluggishness of diffusion, convection and mechanical segregation in viscous siliceous systems. Although the exsolution of an aqueous phase from a silicate melt may substantially increase the rate of diffusion of mobile components, this process also causes more rapid crystallization of the melt (Burnham, 1979), such that it is unlikely that thermogravitational processes operate to any significant degree in high-level magma chambers that cool and crystallize rapidly (Stormer and Whitney, 1985). Additionally, isotopic data indicate that compositional zoning in some large ash flows may be attributable to contamination (Tegtmeyer and Farmer, 1988).

It is perhaps too often that petrologists consider the chamber of crystallization or eruption as the site at which differentiation processes occur. Stormer and Whitney (1985), using feldspar and Fe-Ti oxide equilibria, have shown that silicic magmas, such as the Bishop Tuff, could not have developed their fundamental chemical or mineralogical characteristics in shallow chambers. They believed that differentiation processes controlling composition operated at midcrustal depths. Citing the analogy of the present-day, vertically extensive, igneous activity under the Long Valley caldera, they concluded that zoning in the Bishop Tuff could have originated at depth, with higher level chambers developed just prior to, during and after eruption.

Shannon et al. (1982) and Carten et al. (1988) presented textural evidence and mass-balance calculations indicating that zoning observed in alkali-granite porphyries hosting Climax-type molybdenum deposits probably occurred prior to, or during, emplacement of the small mineralized cupolas into hypabyssal chambers. They postulated that segregation of chemical components occurred by fractionation of a larger body of magma at depth, or during upward transport. Thus, an already-zoned magma was introduced at shallow level, which then began crystallizing from the walls and roof zone toward the core. They argued that concentration of volatiles and mobile metals in the roof zone of the cupolas occurs prior to crystallization of the bulk of the pluton. Flow differentiation in mafic magma chambers has been shown to be a more rapid and effective means of concentrating mineral components than static-chamber processes (Irving, 1978; Irvine, 1979). Recently, Carrigan and Eichelberger (1990) postulated that differences in flow rates of portions of magmas with different viscosities may lead to the injection, or eruption, of zoned magmas. Flow differentiation driven by buoyancy and upward travel through the crust may have played a significant role in the development of zoning observed in the Capitan pluton.

A model of flow differentiation is proposed here whereby viscosity gradients and differential flow rates are developed in the magma as it rises, begins to crystallize and reaches volatile saturation, producing a refractory-mineral-rich porphyry core and a volatile- and mobile-metal-rich roof and margin. Overpressuring brought on by continued crystallization and volatile exsolution caused fracturing of the pluton's roof, which aided in its rapid cooling and development of granophyric texture and veins. Though the directional crystallization textures seen in the Climax porphyries have not been observed in the Capitan pluton, its tabular shape, fine-grained granophyric roof and intrusive-clastic margins are features consistent with rapid, margin-to-core crystallization during, or shortly after, emplacement in a shallow chamber. Further work is necessary to constrain the precise timing and conditions of crystallization, and physical and chemical processes controlling component segregation.

The development of micromiarolites and minor magmatic/hydrothermal REE- and thorium-bearing veins indicates exsolution of an aqueous phase before complete crystallization of the pluton. It is interesting to note that the pluton lacks extensive vein, pegmatite or greisen development. Due to the flat-roofed geometry of the intrusion, rapid crystallization caused dispersion of the vapor phase into micromiarolites and small veins, which inhibited coalescence of the vapor phase into larger vein-stockwork, pegmatite or greisen zones. Perhaps if an equivalent body of magma had intruded in a vertical cylindrical form, rather than a tabular one, greater concentration of volatiles and metals would have occurred, resulting in more economically important mineral deposits.

ACKNOWLEDGMENTS

Tracy A. Delaney provided assistance to the first author in sampling, mapping and petrographic analyses. Conversations with Jim Shannon provided insight into the problems of high-level differentiation apparent in the zoned Capitan pluton. The field assistance provided to the second author by Randy Phillips, Darren Dresser and Andrew Campbell is appreciated. Technical assistance to the second author was provided by Mark Ouimette and Keith Fredzner. We appreciate the helpful reviews by Andrew Campbell and Eugene Foord of an earlier version of this manuscript.

REFERENCES

Aldrich, M. J., Jr., Chapin, C. E. and Laughlin, A. W., 1986, Stress history and tectonic development of the Rio Grande rift, New Mexico: Journal of Geophysical Research, v. 91, no. B6, p. 6199–6211.

Allen, M. S., 1988, The Capitan pluton, New Mexico, an example of a zoned granite magma chamber: Geological Society of America, Abstracts with Programs, v. 20, p. A313.

Allen, M. S. and Foord, E. E., 1991a, The igneous rocks of the Lincoln County porphyry belt, New Mexico: constraints on magma sources and implications: Geological Society of America, Abstracts with Programs, v. 23, p. 2.

Allen, M. S. and Foord, E. E., 1991b, Geochemical and isotopic characteristics of the Lincoln County porphyry belt, New Mexico: implications for regional tectonics and mineral deposits: New Mexico Geological Society, Guidebook 42.

Arth, J. G., 1976, Behavior of trace elements during magmatic processes: a summary of theoretical models and their applications: U.S. Geological Survey, Journal of Research, v. 4, no. 1, p. 41–47.

Baedecker, P. A. and McKown, D. M., 1988, Instrumental neutron activation analysis of geochemical samples; *in* Baedecker, P. A., ed., Methods for geochemical analysis: U.S. Geological Survey, Bulletin 1770, p. H1–H14.

Barker, D. S., 1970, Composition of granophyre, myrmekite, and graphic granite: Geological Society of America Bulletin, v. 81, p. 3339–3350.

Burnham, W., 1979, Magmas and hydrothermal fluids; *in* Barnes, H. L., ed., Geochemistry of hydrothermal ore deposits: New York, Wiley, p. 91–101.

Butler, P., Jr., 1964, Magnetite from intrusives and associated contact deposits, Lincoln County, New Mexico [M.S. thesis]: Socorro, New Mexico Institute of Mining and Technology, 63 p.

Carmichael, I. S. E., Turner, F. J. and Verhoogen, J., 1974, Igneous petrology: New York, McGraw-Hill, 739 p.

Carrigan, C. and Eichelberger, J., 1990, Zoning of magmas by viscosity in volcanic conduits: Nature, v. 343, no. 6255, p. 248–251.

Carten, R. B., Geraghty, E. P., Walker, B. M. and Shannon, J. R., 1988, Cyclic development of igneous features and their relationship to high-temperature hydrothermal features in the Henderson porphyry molybdenum deposit, Colorado: Economic Geology, v. 83, p. 266–296.

Chamberlin, R. M., 1978, Structural development of the Lemitar Mountains: an intrarift tilted fault-block uplift, central New Mexico: 1978 International Symposium on the Rio Grande Rift, Program and Abstracts, Santa Fe, p. 22–24.

Chapin, C. E., 1979, Evolution of the Rio Grande rift: a summary; *in* Riecker, R. E., ed., Rio Grande rift: tectonics and magmatism: Washington, D.C., American Geophysical Union, p. 1–5.

Chapin, C. E., Chamberlin, R. M., Osburn, G. R., White, D. W. and Sanford, A. R., 1978, Exploration framework of the Socorro geothermal area, New Mexico: New Mexico Geological Society, Special Publication 7, p. 115–129.

Chapin, C. E. and Seager, W. R., 1975, Evolution of the Rio Grande rift in Socorro and Las Cruces areas: New Mexico Geological Society, Guidebook 26, p. 297–321.

Craddock, C., 1964, The Lincoln fold system, New Mexico: New Mexico Geological Society, Guidebook 15, p. 122–139.

De la Roche, H., Leterrier, J., Grandclaude, P. and Marchal, M., 1980, A classification of volcanic and plutonic rocks using R_1R_2-diagram and major-element analyses—its relationship with current nomenclature: Chemical Geology, v. 29, p. 183–210.

DePaolo, D. J. and Wasserburg, G. J., 1976, Inferences about magma sources and mantle structure from variations of 143/144 Nd: Geophysical Research Letters, no. 3, p. 743–746.

Dickinson, W. R., 1981, Plate tectonic evolution of the southern Cordillera: Arizona Geological Society Digest, v. 14, p. 113–135.

Dickinson, W. R. and Snyder, W. S., 1978, Plate tectonics of the Laramide Orogeny: Geological Society of America, Memoir 151, p. 355–366.

Farmer, G. L., Broxton, D. E., Warren, R. G. and Pickthorn, W., 1991, Nd, Sr, and O isotopic variations in metaluminous ash flow tuffs and related volcanic rocks at the Timber Mountain/Oasis Valley caldera complex, SW Nevada: implications for the origin and evolution of large volume silicic magma bodies: Contributions to Mineralogy and Petrology, (in press).

Fenn, P. M., 1979, On the origin of graphic intergrowths: Geological Society of America, Abstracts with Programs, v. 11, p. 424.

Fenn, P. M., 1986, On the origin of graphic granite: American Mineralogist, v. 71, p. 325–330.

Geist, D. J., Baker, B. H. and McBirney, A. R., 1985, GPP, a program package for creating and using geochemical data files: Center for Volcanology, University of Oregon, 33 p.

Giles, D. L. and Thompson, T. B., 1972, Petrology and mineralization of a molybdenum-bearing alkalic stock, Sierra Blanca, New Mexico: Geological Society of America Bulletin, v. 83, p. 2129–2148.

Griswold, G. B., 1959, Mineral deposits of Lincoln County, New Mexico: New Mexico Bureau of Mines and Mineral Resources, Bulletin 67, 117 p.

Griswold, G. B., 1964, Mineral resources of Lincoln County: New Mexico Geological Society, Guidebook 15, p. 148–151.

Hanson, G. N., 1978, The application of trace elements to the petrogenesis of igneous rocks of granite composition: Earth and Planetary Science Letters, no. 38, p. 26–43.

Hanson, G. N., 1980, Rare earth elements in petrogenetic studies of igneous systems: Annual Review of Earth and Planetary Science, no. 8, p. 371–406.

Harrer, C. M. and Kelley, V. C., 1963, Reconnaissance of iron resources in New Mexico: U.S. Bureau of Mines, Information Circular 8190, 112 p.

Hildreth, E. W., 1979, The Bishop Tuff: evidence for the origin of compositional zonation in silicic magma chamberss: Geological Society of America, Special Paper 180, p. 43–75.

Irvine, T. N., 1979, Rocks whose composition is determined by crystal accumulation and sorting; *in* Yoder, H. S., ed., The evolution of igneous rocks: Princeton, Princeton University Press, p. 245–306.

Irvine, T. N. and Baragar, W. R. A., 1971, A guide to the chemical classification of the common volcanic rocks: Canadian Journal of Earth Sciences, v. 8, p. 523–548.

Irving, A. J., 1978, Flow crystallization, a mechanism for fractionation of primary magmas at mantle pressures: EOS (Transactions of the American Geophysical Union), v. 59, p. 1214.

Jackson, L. L., Brown, F. W. and Neil, S. T., 1988, Major and minor elements requiring individual determination, classical whole rock analysis, and rapid rock analysis; *in* Baedecker, P. A., ed., Methods for geochemical analysis: U.S. Geological Survey, Bulletin 1770, p. G1–G23.

Johnson, R. G. and King, B. S. L., 1988, Energy dispersive X-ray fluorescence spectrometry; *in* Baedecker, P. A., ed., Methods for geochemical analysis: U.S. Geological Survey, Bulletin 1770, p. F1–F5.

Kelley, V. C., 1949, Geology and economics of New Mexico iron-ore deposits: University of New Mexico Publications in Geology, no. 2, 246 p.

Kelley, V. C., 1952, Origin and pyrometasomatic zoning of the Capitan iron deposits, Lincoln County, New Mexico: Economic Geology, v. 47, p. 64–83.

Kelley, V. C., 1971, Geology of the Pecos country, southeastern New Mexico: New Mexico Bureau of Mines and Mineral Resources, Memoir 24, 75 p.

Kelley, V. C. and Thompson, T. B., 1964, Tectonics and general geology of the Ruidoso-Carrizozo region, central New Mexico: New Mexico Geological Society, Guidebook 15, p. 110–121.

Knapp, R. B. and Norton, D., 1981, Preliminary numerical analysis of processes related to magma crystallization and stress evolution in cooling pluton environments: American Journal of Science, v. 281, p. 35–68.

Lipman, P. W., 1980, Cenozoic volcanism in the western United States: implications for continental tectonics; *in* Studies in geophysics: continental tectonics: Washington, D.C., National Academy of Sciences, p. 161–174.

Lipman, P. W., 1981, Volcano-tectonic setting of Tertiary ore deposits, southern Rocky Mountains: Arizona Geological Society Digest, v. 14, p. 199–213.

Mahood, G. and Hildreth, W., 1983, Large partition coefficients for trace elements in high-silica rhyolites: Geochimica et Cosmochimica Acta, v. 47, p. 11–30.

McBirney, A. R., 1984, Igneous petrology: San Francisco, Freeman, Cooper and Company, 504 p.

McLemore, V. T., 1983, Uranium and thorium occurrences in New Mexico: distribution, geology, production, and resources: New Mexico Bureau of Mines and Mineral Resources, Open-file Report 183.

McLemore, V. T., North, R. M. and Leppert, S., 1988a, Rare-earth elements (REE) in New Mexico: New Mexico Geology, v. 10, p. 33–38.

McLemore, V. T., North, R. M. and Leppert, S., 1988b, Rare-earth elements (REE), niobium and thorium districts and occurrences in New Mexico: New Mexico Bureau of Mines and Mineral Resources, Open-file Report 324, 28 p.

Miller, C. F. and Mittlefehldt, D. W., 1982, Depletion of light rare-earth elements in felsic magmas: Geology, v. 10, p. 129–133.

Moore, S. L., Foord, E. E., Meyer, G. A. and Smith, G. W., 1985, Mineral resources of the Mescalero Apache Indian Reservation, Otero County, New Mexico: U.S. Geological Survey, Administrative Report, 78 p.

Morgan, P., Seager, W. R. and Golombek, M. P., 1986, Cenozoic thermal, mechanical, and tectonic evolution of the Rio Grande rift: Journal of Geophysical Research, v. 91, no. B6, p. 6263–6276.

New Mexico Geological Society, 1982, New Mexico Highway Geologic Map.

Norrish, K. and Hutton, J. J., 1969, An accurate X-ray spectrographic method for the analysis of a wide range of geologic samples: Geochimica et Cosmochimica Acta, v. 33, p. 431–454.

O'Neil, J. R., Shaw, S. E. and Flood, R. H., 1977, Oxygen and hydrogen isotope compositions as indicators of granite genesis in the New England batholith, Australia: Contributions to Mineralogy and Petrology, v. 62, p. 313–328.

Park, D. E., 1971, Petrology of the Tertiary Anchor Canyon stock, Magdalena Mountains, central New Mexico [M.S. thesis]: Socorro, New Mexico Institute of Mining and Technology, 92 p.

Patton, L. T., 1951, Igneous rocks of the Capitan quadrangle, New Mexico, and vicinity: American Mineralogist, v. 31, p. 65–70.

Phillips, R. S., 1990, Geochemistry of hydrothermal Th-U-REE quartz/fluorite veins from the Capitan pluton [M.S. thesis]: Socorro, New Mexico Institute of Mining and Technology, 202 p.

Phillips, R. S., Campbell, A. R. and McLemore, V. T., 1990, Geochemistry of magmatic REE-Th-U quartz/fluorite veins from the Capitan pluton, Capitan Mountains, south-central New Mexico: Geological Society of America, Abstracts with Programs, v. 22, p. A159.

Phillips, R. S. and McLemore, V. T., 1989, Mineralogy and geochemistry of veins in the Capitan Mountains, central New Mexico: New Mexico Geology, v. 12.

Price, J. G., Henry, C. D., Barker, D. S. and Parker, D. F., 1987, Alkalic rocks of contrasting tectonic settings in Trans-Pecos Texas: Geological Society of America, Special Paper 215, p. 335–346.

Renault, J., 1970, Major-element variations in the Potrillo, Carrizozo, and McCartys Basalt Fields, New Mexico: New Mexico Bureau of Mines and Mineral Resources, Circular 113, 22 p.

Segerstrom, K. and Ryberg, G. E., 1974, Geology and placer gold deposits of the Jicarilla Mountains, Lincoln County, New Mexico: U.S. Geological Survey, Bulletin 1308, 25 p.

Shand, S. J., 1922, The problem of the alkaline rocks: Proceedings of the Geological Society of South Africa, no. 25, p. 16–33.

Shannon, J. R., Walker, B. M., Carten, R. B. and Geraghty, E. P., 1982, Unidirectional solidification textures and their significance in determining relative ages of intrusions at the Henderson Mine, Colorado: Geology, v. 10, p. 293–297.

Shaw, G. H., 1974, Phase transitions, elasticity-density relations, and the univalent halides: Journal of Geophysical Research, v. 79, p. 2635–2642.

Sheridan, M. J., 1947, Lincoln County iron deposits, New Mexico: U.S. Bureau of Mines, Report of Investigations 3988, 19 p.

Sidwell, R., 1946, Sediments from alaskite, Capitan Mountains, New Mexico: Journal of Sedimentary Petrology, v. 16, p. 121–123.

Stewart, J. H. and Carlson, J. E., 1978, Generalized maps showing distribution, lithology and age of Cenozoic igneous rocks in the western United States: Geological Society of America, Memoir 152, p. 263–264.

Stormer, J. C., Jr. and Whitney, J. A., 1985, Two feldspar and iron-titanium oxide equilibria in silicic magmas and the depth of origin of large volume ash-flow tuffs: American Mineralogist, v. 70, p. 52–64.

Swanson, S. E., 1976, Relation of nucleation and crystal-growth rate to the development of granitic textures: American Mineralogist, v. 62, p. 966–978.

Taggart, J. E., Jr., Lindsay, J. R., Scott, B. A., Vivit, D. V., Bartel, A. J. and Stewart, K. C., 1988, Analysis of geologic materials by wavelength-dispersive X-ray fluorescence spectrometry; *in* Baedecker, P. A., ed., Methods for geochemical analysis: U.S. Geological Survey, Bulletin 1770, p. E1–E19.

Tegtmeyer, K. and Farmer, G. L., 1988, Nd isotopic gradients in large volume peralkaline rhyolites: evidence for wall rock interaction in upper crustal magma chambers: Geological Society of America, Abstracts with Programs, v. 20, p. A249.

Thompson, T. B., 1972, Sierra Blanca igneous complex, New Mexico: Geological Society of America Bulletin, v. 83, p. 2341–2356.

Tuftin, S. E., 1984, Mineral investigation of the Capitan Mountains Wilderness Area, Lincoln County, New Mexico: U.S. Bureau of Mines, MLA 20-84, 20 p.

Weber, R. H., 1964, Geology of the Carrizozo Quadrangle, New Mexico: New Mexico Geological Society, Guidebook 15, p. 100–109.

Weber, R. H. and Bassett, W. H., 1963, K-Ar ages of Tertiary volcanic and intrusive rocks in Socorro, Catron, and Grant Counties, New Mexico, in Socorro region: New Mexico Geological Society, Guidebook 14, p. 220–223.

White, A. J. R. and Chappell, B. W., 1977, Ultrametamorphism and granitoid genesis: Tectonophysics, v. 43, p. 7–22.

Willis, M. A., Campbell, A. and Phillips, R., 1989, High salinity fluids associated with allanite mineralization, Capitan Mountains, New Mexico: Geological Society of America, Abstracts with Programs, v. 21, p. A287.

Winkler, H. G. F., Boese, M. and Marcopoules, T., 1975, Low temperature granitic melts: Neues Jahrbuch für Mineralogie, Monatshefte, v. 6, p. 245–268.

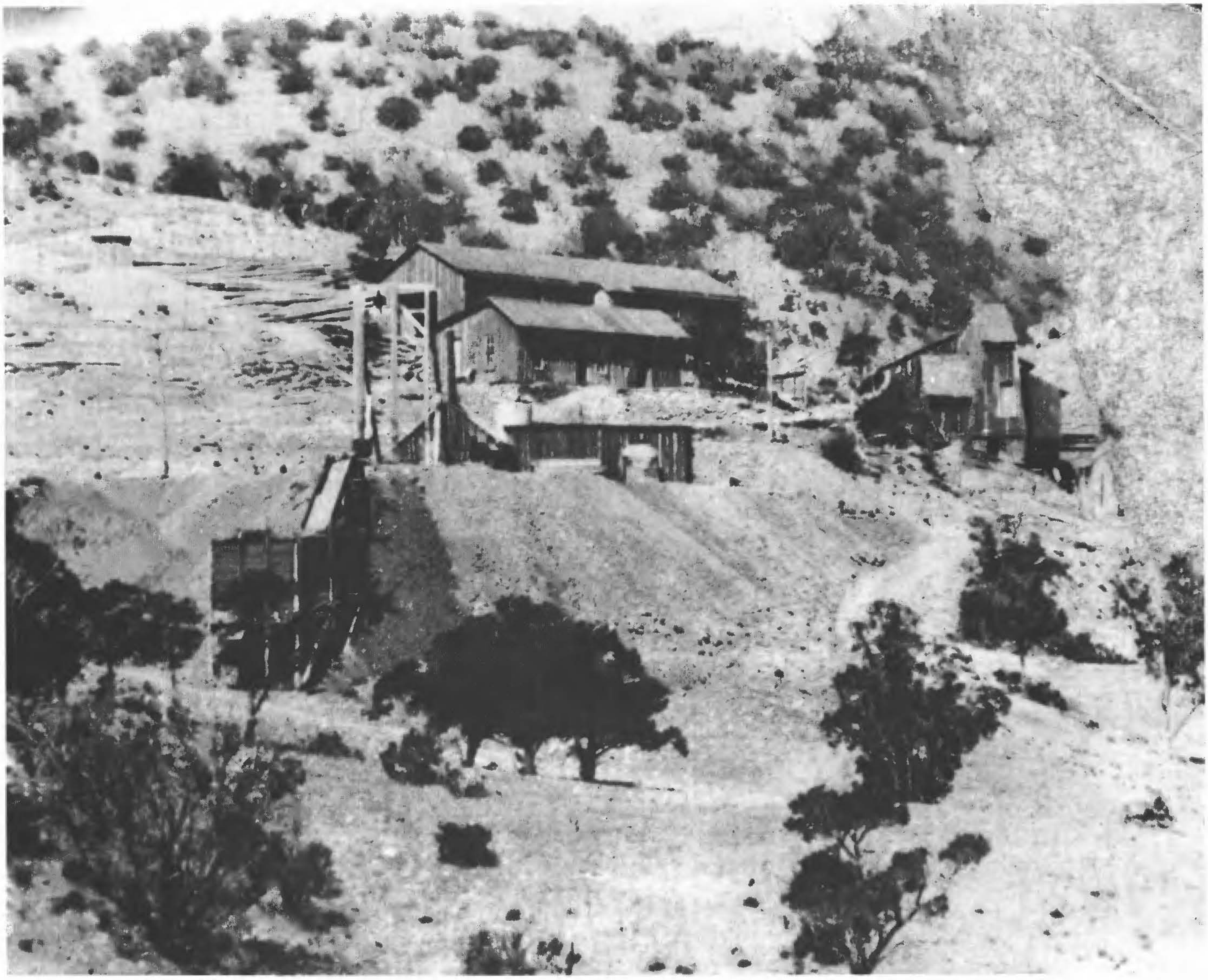

North Homestake mine, White Oaks mining district, circa 1913. This rare but badly damaged view taken well after the zenith of gold production, shows the North Homestake shaft at far right, miners' change room and carpenter shop in center. In the foreground, center and left, are the engine house, headframe and ore bins of the Rita mine. Both properties would again flourish, albeit briefly, during the tungsten boom beginning about 1915. New Mexico Bureau of Mines collection No. 1663, courtesy of Richard H. Jahns and John Kelt.